SCIENCE CHINA
Physics, Mechanics & Astronomy

• Article •

December 2012 Vol.55 No.12: 2407–2413
doi: 10.1007/s11433-012-4922-3

The effect of symmetry potential on the balance energy of light particles emitted from mass symmetric heavy-ion collisions with isotopes, isobars and isotones

WANG YongJia[1,2], GUO ChenChen[1,3], LI QingFeng[1*] & ZHANG HongFei[2]

[1] *School of Science, Huzhou Teachers College, Huzhou 313000, China;*
[2] *School of Nuclear Science and Technology, Lanzhou University, Lanzhou 730000, China;*
[3] *College of Nuclear Science and Technology, Beijing Normal University, Beijing 100875, China*

Received August 27, 2012; accepted October 17, 2012; published online November 21, 2012

Using the Ultrarelativistic Quantum Molecular Dynamics (UrQMD) model, the balance energies of free neutrons, free protons and Z=1 particles (including free protons, deuterons and tritons) from mass symmetric heavy-ion collisions with isotopes, isobars and isotones are studied. The influence of nuclear symmetry potential energy on the balance energy is emphasized. It is found that the balance energy of free neutrons is sensitive to the nuclear symmetry energy, while that of free protons is not. Particularly, the initial neutron/proton ratio dependence of the balance energy of free neutrons from Sn isotopes can be taken as a useful probe to constrain the stiffness of the nuclear symmetry energy.

symmetry energy, directed flow, balance energy

PACS number(s): 21.65.Ef, 25.70.-z, 25.75.Ld

Citation: Wang Y J, Guo C C, Li Q F, et al. The effect of symmetry potential on the balance energy of light particles emitted from mass symmetric heavy-ion collisions with isotopes, isobars and isotones. Sci China-Phys Mech Astron, 2012, 55: 2407–2413, doi: 10.1007/s11433-012-4922-3

1 Introduction

One of the researched areas in heavy ion collisions (HICs) at the incident energies from 40 to 400 MeV/nucleon is to study the density dependence of the symmetry energy included in the nuclear equation of state (EoS), which is defined as the difference in energy per nucleon between the pure neutron matter and the isospin symmetric nuclear matter. It is well known that the symmetry energy is critical for many aspects not only in nuclear physics, e.g., nuclear masses, neutron skin thickness of nuclei [1,2] and the structure of exotic nuclei, but also in astrophysics, e.g., supernova dynamics, and the structure of neutron stars (their masses and radii) [3]. Significant progress has been made in recent years in constraining the density dependence of the symmetry energy, a number of useful probes have been proposed as well, particularly around and below the saturation density. Nevertheless, the high density behavior of the nuclear symmetry energy is still not well constrained partly because of the strong model dependence. For recent review we refer the reader to refs. [4,5].

The nuclear collision offers a unique opportunity to investigate the EoS of compressed, hot and isospin asymmetric nuclear matter. The collective flow is a common phenomenon from nuclear collisions, which was first discovered at Bevalac in 1984 and has been widely studied since then (see, e.g., ref. [6], and references therein). Different components of the collective flow have been used frequently to constrain the stiffness of the EoS [7]. In recent years, to further constrain the stiffness of the symmetry energy has become one of the major interests in the exploration of in-

*Corresponding author (email: liqf@hutc.zj.cn)

termediate energy HICs. But, since the effect of the symmetry energy on the collective flow is relatively weak and even further interfered by uncertainties in the in-medium nucleon-nucleon collisions as well as various model parameters, it becomes difficult to pin down thoroughly the behavior of symmetry energy directly from the collective flow. Recently, it was found that the neutron-proton differential transverse flow [4,8], the neutron-proton elliptic flow difference [9], and the ratio of the elliptic flow parameters of neutrons with respect to protons or hydrogen isotopes [10], can be taken as sensitive observables to the density dependence of the symmetry energy. Certainly, to more strictly constrain the symmetry energy, one needs more precisely experimental data as well as more self-consistently theoretical models.

The directed and elliptic flows are two popular flow components which are extracted from the Fourier expansion of the azimuthal distributions of emitted particles with respect to the reaction plane. Previous studies of the beam-energy dependence of the directed flow showed that the slope of the directed flow at mid-rapidity changes sign from negative to positive at an incident energy, termed as the balance energy ($E_{\rm bal}$). It was soon later found that this is the result of the balance between the attractive mean-field potentials and the repulsive binary collisions. This interesting phenomenon has been widely detected by many experiments during the last two decades (see refs. [11–16] and references therein). Theoretical studies with the help of transport models have demonstrated that the $E_{\rm bal}$ is sensitive to the nuclear EoS, the in-medium cross section [17–25], and the momentum dependence of the interactions [13,20, 26]. But, in early studies, it was reported that the $E_{\rm bal}$ does not heavily depend on the emitted particle species [13,15]. In most of these theoretical investigations one particle independent global quantity "directed transverse momentum $\left\langle p_X^{\rm dir} \right\rangle$" was taken into use. However, more recent experimental data for the ^{197}Au+^{197}Au system published by the INDRA-ALADIN collaboration have shown clearly that the slope of directed flow changes the sign at about 60 MeV/nucleon for Z=2 particles, but it moves to be about 80 MeV/nucleon for Z=1 particles [27].

The isospin dependence of $E_{\rm bal}$ has been studied theoretically with the isospin-dependent quantum molecular dynamics (IQMD) model [17,28], the Boltzmann-Nordheim-Vlasov (BNV) model [29] and the isospin-dependent Boltzmann-Uehling-Ulenbeck (IBUU) model [14]. Experimentally, the $E_{\rm bal}$ values for ^{58}Fe+^{58}Fe and ^{58}Ni+^{58}Ni have been measured by MSU 4π Array, and shown that it depends on the isospin of the system, which is basically in agreement with the prediction of the isospin-dependent BUU model [14]. However, it can be noted that the measured values of $E_{\rm bal}$ were extracted from the transverse flow of Z=2 fragments, while the calculated values were only for nucleons. The $E_{\rm bal}$ for these two reactions were studied more widely at various conditions with different theoretical models [19,28–30]. Although all these studies shown that the $E_{\rm bal}$ for these two reactions are different, calculations of the $E_{\rm bal}$ value were performed not to depend on emitted particle species. Thus, it is quite necessary to further investigate the isospin effect on the $E_{\rm bal}$ for different particle species emitted from systems with different initial isospin.

In our recent work, the system-mass and particle-species dependence of $E_{\rm bal}$ was investigated [31]. It was shown that the $E_{\rm bal}$ of free neutrons from HICs is sensitive to the density dependence of the symmetry potential energy. In this work, we further examine the isospin effect on $E_{\rm bal}$ by taking several groups of semicentral (with reduced impact parameters b_0=b/$b_{\rm max}$=0.15–0.4, where $b_{\rm max}$ is the sum of the radii of the colliding nuclei) collisions of isotopes (^{100}Sn+^{100}Sn, ^{112}Sn+^{112}Sn, ^{124}Sn+^{124}Sn, ^{132}Sn+^{132}Sn), isobars (^{132}Xe+^{132}Xe, ^{132}Ce+^{132}Ce, ^{132}Sm+^{132}Sm) and isotones (^{124}Sn+^{124}Sn, ^{132}Ce+^{132}Ce, ^{140}Dy+^{140}Dy) into account.

The paper is organized as follows. In the following section, the symmetry energy used in the updated version of the Ultrarelativistic Quantum Molecular Dynamics (UrQMD) model is given. The appearance and the time evolution of the directed flow is vividly demonstrated as well. Also, we calculate the $E_{\rm bal}$ of free protons, Z=1 particles and free neutrons, calculation results of the isospin dependent $E_{\rm bal}$ are shown and analyzed in details.

2 Density-dependent symmetry energy and directed flow

The density-dependent symmetry energy used in this work is expressed as:

$$
\begin{aligned}
E_{\rm sym} &= E_{\rm sym}^{\rm pot} + E_{\rm sym}^{\rm kin} \\
&= 20\ {\rm MeV} \cdot (\rho/\rho_0)^{\gamma} + 12\ {\rm MeV} \cdot (\rho/\rho_0)^{2/3}, \qquad (1)
\end{aligned}
$$

where the coefficient γ in the potential part $E_{\rm sym}^{\rm pot}$ is the corresponding strength parameter, and ρ and ρ_0 in the $E_{\rm sym}^{\rm pot}$ and the Fermi kinetic energy $E_{\rm sym}^{\rm kin}$ are nuclear density and normal nuclear density, respectively.

In addition, we choose a soft EoS with momentum dependence (SM-EoS, corresponding incompressibility K= 200 MeV) and a momentum- and density-modified nucleon-nucleon elastic cross section which were examined in our recent work [32]. It was found that, at INDRA/GSI energies (40–150 MeV/nucleon), the slope of directed flow of Z=1 particles at midrapidty can be reproduced rather well with this parameter set.

The time evolution of the nuclear densities in the central zone (with in a cube of length 4 fm) of ^{100}Sn+^{100}Sn, ^{132}Sn+^{132}Sn and ^{132}Sm+^{132}Sm reactions at 85 MeV/nucleon and b_0=0.3 is shown in Figure 1. The symmetry potential

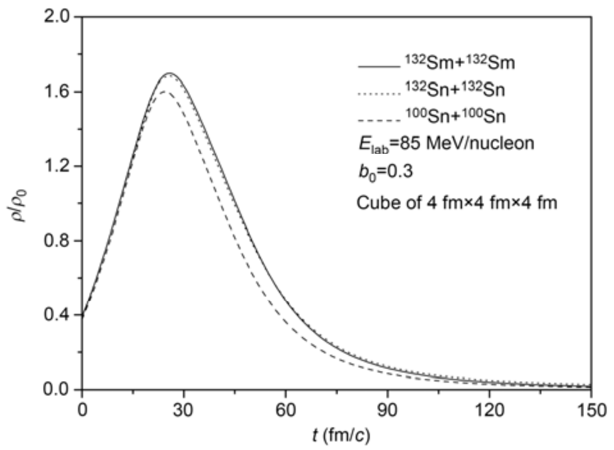

Figure 1 Time evolution of central nuclear densities for ^{100}Sn+^{100}Sn, ^{132}Sn+^{132}Sn and ^{132}Sm+^{132}Sm reactions at $E_{\rm lab}$=85 MeV/nucleon and b_0=0.3.

strength parameter γ=1.0 is used in calculations. It is seen that the maximum density is about 1.7 times of normal one, and is weakly influenced by the initial N/Z ratio of the colliding system (when the total mass numbers are the same), which is reasonable. Furthermore, the supra-normal density nuclear matter is built up within the time span from about 15 fm/c to 45 fm/c in this beam energy region. Afterwards, the system decompresses.

During the same process, the flow appears and evolves. In upper plots of Figure 2 the contour plots (in the x-z plane) of the density of all protons from semi-central ^{132}Sn+^{132}Sn collisions at 85 MeV/nucleon and at three time points (0 fm/c (a), 30 fm/c (b), and 150 fm/c (c)) are shown. Correspondingly, the momentum p_x-p_z distributions of all protons at the three times are shown in lower plots (Figures 2(d), (e), and (f)). 8000 events are collected in the calculation. Figures 2(a) and (d) denotes the initialization of the two nuclei, and sampled target and projectile nuclei are surely same in the phase space, the average value of p_x in each p_z bin (shown by the line in Figure 2(d)) clearly shows no initial flow as well. At t=30 fm/c (in Figures 2(b) and (e)), when the maximum density is made in the central zone of the colliding system, a negative directed flow is formed, which is due to the dominance of the attractive mean-field potentials compared to the repulsive binary collisions. At the end of the collision, i.e., 150 fm/c (in Figures 2(c) and (f)), the negative directed flow is largely reduced due to the well known binary rescattering process.

The directed flow is commonly expressed as v_1, which is one of coefficients of the azimuthal distribution of the emitted particles [33],

$$\frac{\mathrm{d}N}{\mathrm{d}\phi} = v_0[1 + 2v_1\cos(\phi) + 2v_2\cos(2\phi)], \quad (2)$$

and

$$v_1 \equiv \langle \cos(\phi) \rangle = \left\langle \frac{p_x}{p_{\rm t}} \right\rangle, \quad (3)$$

where ϕ is the azimuthal angle of the emitted particle with respect to the reaction plane, and the angle brackets denote

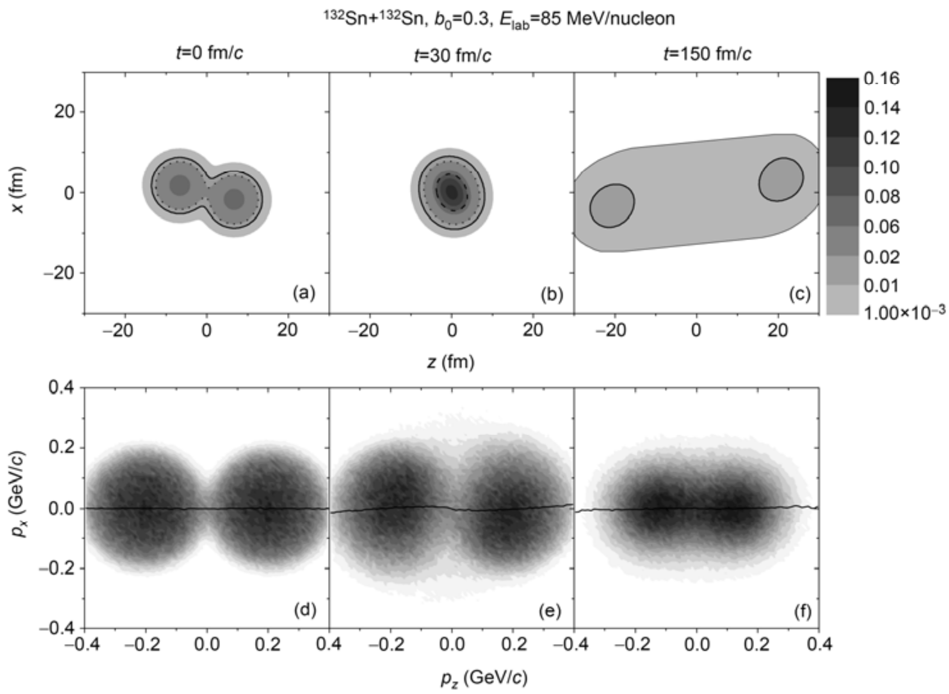

Figure 2 Upper: Contour plots of the density of all protons in the reaction plane of semi-central ^{132}Sn+^{132}Sn collisions at 85 MeV/nucleon and at three times (0 fm/c (a), 30 fm/c (b), and 150 fm/c (c)). The solid, dotted and dashed lines represent the boundary of ρ_0/16, ρ_0/8, and ρ_0/2, respectively. Lower: Corresponding momentum distributions at same times in (d), (e), (f), respectively. The line in each plot denotes the average value of p_x for every p_z bin.

an average over all considered particles from all events, and $p_t = \sqrt{p_x^2 + p_y^2}$ is the transverse momentum. For a certain reaction, the directed flow is functions of p_t and normalized longitudinal rapidity $y_0=y_z/y_{pro}$, where y_{pro} is the projectile rapidity in the center-of-mass system. For symmetric collisions, $\langle \cos\phi \rangle$ is an odd function of the center-of-mass rapidity, leading to the well-known "S-shape" of v_1 as a function of rapidity [33]. The variation of v_1 with y_0, can be well fitted by $v_1(y_0) = \kappa y_0 + b y_0^3 + c$, where κ is the slope of v_1 at mid-rapidity (y_0=0). If $\kappa>0$ ($\kappa<0$), it indicates that the directed flow is positive (negative). When $\kappa=0$, it represents that the directed flow disappears, and the corresponding incident energy is termed balance energy. For the method to quantitatively determine the E_{bal}, we refer the reader to ref. [31].

3 Results

Figure 3 depicts the dependence of the E_{bal} of free neutrons (top (a), (b), and (c) plots), Z=1 particles (middle (d), (e), and (f) plots) and free protons (bottom (g), (h), and (i) plots) on the initial N/Z ratio from semi-central and mass-symmetric HICs with isotopes (^{100}Sn+^{100}Sn, ^{112}Sn+^{112}Sn, ^{124}Sn+^{124}Sn, ^{132}Sn+^{132}Sn, left plots), isobars (^{132}Xe+^{132}Xe, ^{132}Ce+^{132}Ce, ^{132}Sm+^{132}Sm, ^{132}Sn+^{132}Sn, middle plots) and isotones (^{124}Sn+^{124}Sn, ^{132}Ce+^{132}Ce, ^{140}Dy+^{140}Dy, right plots). Calculations with the consideration of the symmetry energy and with different γ parameters are shown by lines with solid symbols, while cases without the consideration of both Coulomb and symmetry potentials are shown with dotted lines with open circles. We simulate 600 thousand events for each reaction at incident energies around its balance energy in steps of 2 MeV/nucleon, then the E_{bal} can be extracted with high accuracy (errors are within about 1 MeV).

Firstly, from Figure 3, it can be seen clearly that for all colliding systems under consideration the influence of symmetry potential with different values of γ on the E_{bal} for free neutrons is the strongest of all, while the values of E_{bal} for free protons keep almost no change when varying the value of γ. It is similar to calculations in ref. [31] for Au+Au reactions.

Secondly, from Figures 3(a)–(c), it can be also observed that the value of E_{bal} of free neutrons changes almost linearly with the increase of the N/Z ratio and the influence of symmetry energy on E_{bal} becomes stronger with larger value of the N/Z ratio. Particularly, the E_{bal} of free neutrons in Figure 3(a) slightly increases with increasing both mass number and N/Z ratio when the soft (γ=0.5) symmetry potential energy is chosen, the corresponding slope parameters κ equals 5.5±0.6. It becomes flat (κ=0.7±0.9) when γ=1.0, and starts to decrease (κ=–2.5±0.4) when γ=1.5. Therefore, the E_{bal} of free neutrons from mass symmetric HICs with Sn isotopes can be taken as a sensitive probe to complementarily constrain the density dependence of symmetry potential energy. Recently, Sood [17] studied N/Z and N/A dependence of E_{bal} for isotopic series of a lighter system, Ca+Ca, within IQMD model, and also claimed that the N/Z and N/A dependence of E_{bal} are sensitive to the symmetry energy. More specifically, we found that this probe mainly provides the information of the symmetry energy at supra-normal densities since the values of the balance energy of free neutrons calculated with the soft symmetry energy

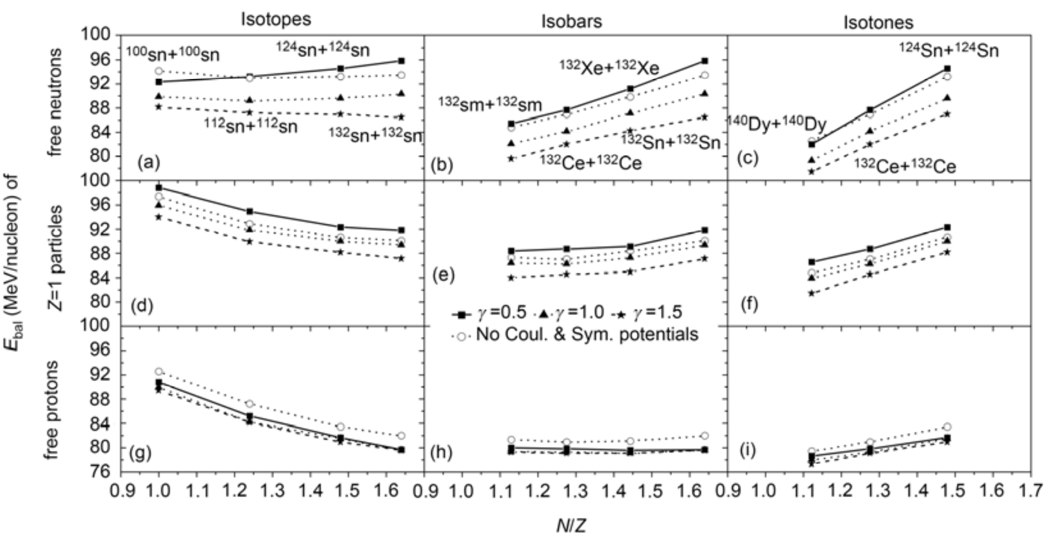

Figure 3 N/Z dependent balance energies of free neutrons (top plots), Z=1 particles (middle plots) and free protons (bottom plots) for semi-central (b_0 =0.15–0.4) and mass-symmetric HICs with isotopes (left plots), isobars (middle plots), and isotones (right plots). Calculations with different strength parameters γ=0.5, 1.0, and 1.5 are shown by lines with solid symbols, while the dotted lines with open circles are calculations without both symmetry and Coulomb potentials.

are higher than those with the hard one (although the sensitivity is largely reduced by the symmetry potential in the sub-normal density region especially at the late stage) [31]. It is known that at supra-normal densities a soft symmetry potential will cause weaker repulsion (attraction) for neutrons (protons) in the neutron-rich fireball than a stiff symmetry potential, which leads to higher value of the balance energy. We further find that, if both Coulomb and symmetry potentials are switched off, the values of $E_{\rm bal}$ are monotonously driven up when compared to results with a linear symmetry potential energy. It is a result of both the repulsive symmetry potential for neutrons in neutron-rich system and the repulsive Coulomb potential for protons in any system.

Lastly, if we observe from Figure 3(a) to Figure 3(b), it can be found that the $E_{\rm bal}$ of free neutrons with all γs increase with increasing N/Z for isobaric systems. It is because that for more neutron-rich system, the total binary collision number decreases due to the facts that both neutron-neutron and proton-proton elastic cross sections are smaller than neutron-proton one and, the Pauli blocking effect on neutron-neutron collisions becomes stronger. If we further move to Figure 3(c), it is seen that the $E_{\rm bal}$ of free neutrons rise more quickly with increasing N/Z since now the isotones become smaller. With the decrease of the total mass number of the colliding system, the average collision number for each nucleon should be decreased as well. Therefore, we can conclude that the $E_{\rm bal}$ of free neutrons increases with increasing N/Z, and decreases with increasing system mass. The effects cancel each other to a large extent in isotopic systems shown in Figure 3(a). This cancellation makes it possible to enlarge the symmetry potential effect on the $E_{\rm bal}$. However, for free protons, the weak N/Z and symmetry potential dependence of the $E_{\rm bal}$ shown in Figure 3(h) implies that it is dominantly affected by the size but not by the isospin of the system. The fall and rise of the $E_{\rm bal}$ of free protons shown in Figures 3(g) and (i), respectively, are mainly due to the change of the total mass number of systems.

From Figures 3(a), (d), and (g), it can be noted that, even for the isospin-symmetric system (^{100}Sn+^{100}Sn), the influence of γ values on the $E_{\rm bal}$ of free neutrons and Z=1 particles is still large, which is due to the non-equilibrium dynamic evolution of the local isospin asymmetry ($\delta=(\rho_{\rm n}-\rho_{\rm p})/(\rho_{\rm n}+\rho_{\rm p})$). Figure 4 illustrates the contour plots of δ in the reaction plane of semi-central ^{100}Sn+^{100}Sn collisions at $E_{\rm lab}$=85 MeV/nucleon and at time points 30 fm/c (a), 60 fm/c (b), 90 fm/c (c), and 150 fm/c (d). From Figure 1, we know that at approximately 30 fm/c, the nuclear density in the central region is up to 1.5 times of nuclear normal density, and it can be seen from Figure 4(a) that δ is positive in the central region of the fireball. Concurrently, it is negative in the peripheral region of the fireball. It is primarily due to the repulsive Coulomb force which makes protons more difficult to be compressed than neutrons. As the reaction continues, the isospin asymmetry becomes even more obvious in the neck region which is so-called the isospin distillation and has already been investigated by other people [34,35].

The different sensitivities to the isospin shown in Figures 3(b), (e), and (h) can also be better understood by comparing the time evolution of two typical systems, ^{132}Sn+^{132}Sn

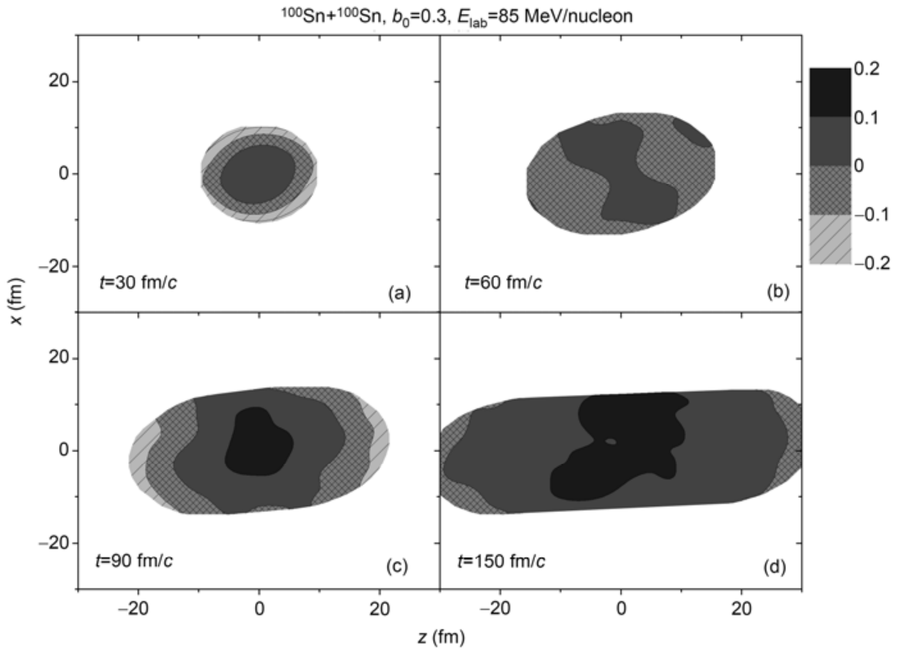

Figure 4 Contour plots of the isospin asymmetry δ in the reaction plane of semi-central (b_0=0.3) ^{100}Sn+^{100}Sn collision at $E_{\rm lab}$=85 MeV/nucleon and at time points 30 fm/c (a), 60 fm/c (b), 90 fm/c (c), and 150 fm/c (d). γ=1.0 is chosen in calculations. δ will be shown only if both the neutron ($\rho_{\rm n}$) and proton ($\rho_{\rm p}$) densities are greater than 0.001 fm^{-3}.

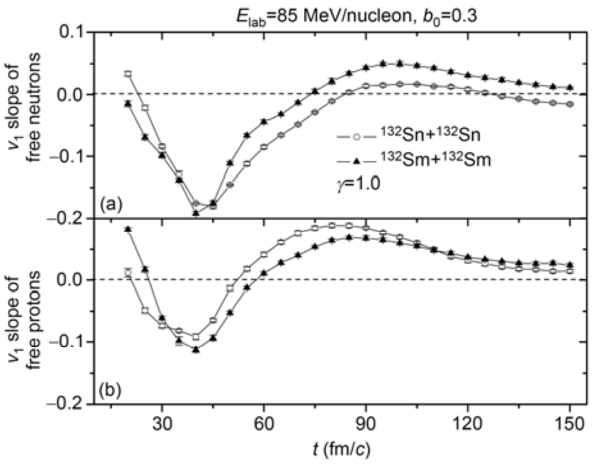

Figure 5 Time evolution of the slope of directed flow v_1 for free neutrons (a) and free protons (b) from ^{132}Sn+^{132}Sn (lines with circles) and ^{132}Sm+^{132}Sm (lines with triangles) collisions at E_{lab}=85 MeV/nucleon and b_0=0.3. γ=1.0 is chosen in calculations.

and ^{132}Sm+^{132}Sm. Figure 5 shows the time evolution of slopes of the directed flow v_1 at mid-rapidity for free neutrons (a) and free protons (b) from these two collisions at 85 MeV/nucleon and b_0=0.3. It is apparent that the total process may be divided into three time spans: with time increasing, and 1) at $t \lesssim 40$ fm/c, the v_1 slopes decrease quickly; 2) at $40 \lesssim t \lesssim 90$ fm/c, the v_1 slopes increase quickly; 3) at $t \lesssim 90$ fm/c, the v_1 slopes decrease again but slowly. In the first period, the system compresses and the attractive mean field dominates so that the v_1 slope decreases and changes to negative at such a beam energy. In the second period, the system starts to decompress and the two-body repulsive rescattering plays a more important role than the net contribution of the mean field. In the last period, collisions between nucleons almost cease and the residual interactions including both Coulomb and nuclear forces influence weakly the emission of clusters. Although the Coulomb potential contributes a repulsion to the flow of protons, the decrease of the v_1 slope shown in Figure 5(b) implies that the net contribution of potentials is still attractive.

Further, if we compare the result of ^{132}Sn+^{132}Sn with that of ^{132}Sm+^{132}Sm, we may find two interesting phenomena. The first one is the crossing behavior at t=30–40 fm/c. Before this time, the v_1 slope of free neutrons from ^{132}Sn+^{132}Sn reactions is larger than that from ^{132}Sm+^{132}Sm reactions which is primarily because of the repulsion of the symmetry potential on neutrons in the neutron-rich ^{132}Sn+^{132}Sn system. For the v_1 slope of free protons, contrarily, the result from ^{132}Sm+^{132}Sm reactions is larger than that from ^{132}Sn+^{132} Sn reactions, which is due to both a stronger repulsion of the Coulomb potential and a weaker attraction of the symmetry potential in the ^{132}Sm+^{132}Sm system. After this time, however, since the two-body collision starts to have a more important role, the collision number per nucleon controls the slope of flow. The v_1 slope of free protons from ^{132}Sn+^{132}Sn reactions starts to be larger than that from ^{132}Sm+^{132}Sm reactions only because protons in the neutron-rich system have more chance to collide with neutrons than with protons, and it is known that neutron-proton elastic cross section is larger than proton-proton (neutron-neutron). This hold also for the v_1 slope of free neutrons. The second interesting behavior in the comparison of the results from the two systems comes from the late stage of the whole process. That is, the difference of v_1 slope of free protons between the two systems almost disappears while that of neutrons survives in the end of the process. For protons, a stronger Coulomb potential in ^{132}Sm+^{132}Sm reactions leads to a weaker decrease of the v_1 slope than in ^{132}Sn+^{132}Sn reactions so that both of them meet together in the end. For neutrons, it does not occur because the Coulomb potential does not work on neutrons.

4 Summary

To summarize, within the improved version of UrQMD model, the balance energies of free neutrons, Z=1 particles and free protons from mass symmetric HICs with isotopes, isobars and isotones are investigated. The influence of symmetry energy on the balance energy is emphasized. It is shown that the balance energy of free neutrons follows a linear behavior as a function of the initial N/Z ratio of the colliding system, and is sensitive to the nuclear symmetry energy. Particularly, the initial N/Z dependence of the balance energy of free neutrons from Sn isotopes can be taken as a useful probe to constrain the stiffness of the nuclear symmetry energy. We also found that in reactions with isobars (here A=132), the balance energy of free neutrons increases with the increase of the initial N/Z ratio, but that of free protons almost does not depend on the initial N/Z of the system.

We acknowledge support by the computing server C3S2 in Huzhou Teachers College. The work was supported by the National Natural Science Foundation of China (Grant Nos. 10905021, 10979023 and 11175074), the Zhejiang Provincial Natural Science Foundation of China (Grant No. Y6090210) and the Qian-Jiang Talents Project of Zhejiang Province (Grant No. 2010R10102).

1 Warda M, Vinas X, Roca-Maza X, et al. Neutron skin thickness in droplet model with surface width dependence: Indications of softness of the nuclear symmetry energy. Phys Rev C, 2009, 80: 024316
2 Chen L W, Ko C M, Li B A. Nuclear matter symmetry energy and the neutron skin thickness of heavy nuclei. Phys Rev C, 2005, 72: 064309; Chen L W. Higher order bulk characteristic parameters of asymmetric nuclear matter. Sci China-Phys Mech Astron, 2011, 54: s124–s129; Tian W D, Ma Y G, Cai X Z, et al. Isospin and symmetry energy study in nuclear EOS. Sci China-Phys Mech Astron, 2011, 54: s141–s148
3 Steiner A W, Prakash W, Lattimer J M, et al. Isospin asymmetry in nuclei and neutron stars. Phys Rep, 2005, 411: 325–375
4 Li B A, Chen L W, Ko C M. Recent progress and new challenges in isospin physics with heavy-ion reactions. Phys Rep, 2008, 464:

113–281
5 Shetty D V, Yennello S J. Nuclear symmetry energy: An experimental overview. Pramana, 2010, 75: 259–270
6 Reisdorf W, Ritter H G. Collective flow in heavy-ion collisions. Ann Rev Nucl Part Sci, 1997, 47: 663–709
7 Danielewicz P, Lacey R, Lynch W G. Determination of the equation of state of dense matter. Science, 2002, 298: 1592–1596
8 Li B A. Neutron proton differential flow as a probe of isospin dependence of nuclear equation of state. Phys Rev Lett, 2000, 85: 4221–4224
9 Cozma M D. Neutron-proton elliptic flow difference as a probe for the high density dependence of the symmetry energy. Phys Lett B, 2011, 700: 139–144
10 Russotto P, Wu P Z, Zoric M, et al. Symmetry energy from elliptic flow in ^{197}Au +^{197}Au. Phys Lett B, 2011, 697: 471–476
11 Magestro D J, Bauer W, Bjarki O, et al. Disappearance of transverse flow in Au+Au collisions. Phys Rev C, 2000, 61: 021602(R)
12 Ogilvie C A, Bauer W, Cebra D A, et al. Disappearance of flow and its relevance to nuclear matter physics. Phys Rev C, 1990, 42: R10–R14
13 Pak R, Bjarki O, Hannuschke S A, et al. Momentum dependence of the nuclear mean field from peripheral heavy-ion collisions. Phys Rev C, 1996, 54: 2457–2462
14 Pak R, Li B A, Benenson W, et al. Isospin dependence of the balance energy. Phys Rev Lett, 1997, 78: 1026–1029
15 Westfall G D, Bauer W, Craig D, et al. Mass dependence of the disappearance of flow in nuclear collisions. Phys Rev Lett, 1993, 71: 1986–1989
16 INDRA collaboration. Measurements of sideward flow around the balance energy. Phys Rev C, 2002, 65: 044604
17 Sood A D. *N*/*Z* and *N*/*A* dependence of balance energy as a probe of symmetry energy in heavy-ion collisions. Phys Rev C, 2011, 84: 014611
18 Gautam S, Sood A D. Isospin effects on the mass dependence of balance energy. Phys Rev C, 2010, 82: 014604
19 Gautam S, Chugh R, Sood A D, et al. Isospin effects on the energy of vanishing flow in heavy-ion collisions. J Phys G, 2010, 37: 085102
20 Chugh R, Puri R K. Importance of momentum dependent interactions at the energy of vanishing flow. Phys Rev C, 2010, 82: 014603
21 Goyal S. Role of colliding geometry on the balance energy of mass-asymmetric systems. Phys Rev C, 2011, 83: 047604
22 Gautam S, Sood A D, Puri R K. Isospin effects in the disappearance of flow as a function of colliding geometry. Phys Rev C, 2011, 83: 014603
23 Kumar S, Rajni, Kumar S. Experimental balance energies and isospin-dependent nucleon-nucleon cross-sections. Phys Rev C, 2010, 82: 024610
24 Sood A D, Puri R K. Mass dependence of disappearance of transverse flow. Phys Rev C, 2004, 69: 054612
25 Sood A D, Puri R K, Aichelin J. Disappearance of transverse flow in central collisions for heavier nuclei. Phys Lett B, 2004, 594: 260–264
26 Sood A D, Puri R K. Influence of momentum-dependent interactions on balance energy and mass dependence. Eur Phys J A, 2006, 30: 571–577
27 Andronic A, Łukasik J, Reisdorf W, et al. Systematics of stopping and flow in Au+Au collisions. Eur Phys J A, 2006, 30: 31–46
28 Chen L W, Zhang F S, Jin G M. Analysis of isospin dependence of nuclear collective flow in an isospin-dependent quantum molecular dynamics model. Phys Rev C, 1998, 58: 2283–2291
29 Scalone L, Colonna M, Di T M. Transverse flows in charge asymmetric collisions. Phys Lett B, 1999, 461: 9–14
30 Daffin F, Bauer W. Effects of isospin asymmetry and in-medium corrections on balance energy. arXiv:nucl-th/9809024
31 Guo C C, Wang Y J, Li Q F, et al. In fluence of the symmetry energy on the balance energy of the directed flow. Sci China-Phys Mech Astron, 2012, 55: 252–259
32 Li Q F, Shen C W, Guo C C, et al. Nonequilibrium dynamics in heavy-ion collisions at low energies available at the GSI Schwerionen Synchrotron. Phys Rev C, 2011, 83: 044617
33 Reisdorf W, Leifels Y, Andronic A, et al. Systematics of azimuthal asymmetries in heavy ion collisions in the 1A GeV regime. Nucl Phys A, 2012, 876: 1–60
34 Di T M, Baran V, Colonna M, et al. Probing the nuclear symmetry energy with heavy-ion collisions. J Phys G, 2010, 37: 083101
35 Baran V, Colonna M, Greco V, et al. Reaction dynamics with exotic beams. Phys Rep, 2005, 410: 335–466